

# AuraSense: Enabling Expressive Around-Smartwatch Interactions with Electric Field Sensing

Junhan Zhou<sup>2</sup>   Yang Zhang<sup>1</sup>   Gierad Laput<sup>1</sup>   Chris Harrison<sup>1</sup>

<sup>1</sup>Human-Computer Interaction Institute, <sup>2</sup>Electrical and Computer Engineering Department  
Carnegie Mellon University

5000 Forbes Avenue, Pittsburgh, PA 15213

{yang.zhang, gierad.laput, chris.harrison}@cs.cmu.edu, junhanz@ece.cmu.edu

## ABSTRACT

Existing smartwatches rely on touchscreens for display and input, which inevitably leads to finger occlusion and confines interactivity to a small area. In this work, we introduce AuraSense, which enables rich, around-device, smartwatch interactions using electric field sensing. To explore how this sensing approach could enhance smartwatch interactions, we considered different antenna configurations and how they could enable useful interaction modalities. We identified four configurations that can support six well-known modalities of particular interest and utility, including gestures above the watchface and touchscreen-like finger tracking on the skin. We quantify the feasibility of these input modalities in a series of user studies, which suggest that AuraSense can be low latency and robust across both users and environments.

## Author Keywords

Wearables; Smartwatches; Electric Field Sensing; Around-Device Interaction; ADI.

## ACM Classification Keywords

H.5.2: [User Interfaces]— Input devices and strategies.

## INTRODUCTION

Smartwatches and wearable devices promise to offer enhanced convenience to everyday communication and information retrieval tasks. However, because of their small size, the interfaces they run are often limited and cumbersome. Existing approaches generally rely on the touchscreen for display and input, but this is problematic because it inevitably leads to finger occlusion and confined interactivity. To mitigate this issue, researchers have explored techniques to leverage the area *around* devices to provide an expanded volume for input, often described as “around-device interaction” (ADI).

Permission to make digital or hard copies of all or part of this work for personal or classroom use is granted without fee provided that copies are not made or distributed for profit or commercial advantage and that copies bear this notice and the full citation on the first page. Copyrights for components of this work owned by others than ACM must be honored. Abstracting with credit is permitted. To copy otherwise, or republish, to post on servers or to redistribute to lists, requires prior specific permission and/or a fee. Request permissions from [Permissions@acm.org](mailto:Permissions@acm.org).

UIST 2016, October 16-19, 2016, Tokyo, Japan  
© 2016 ACM. ISBN 978-1-4503-4189-9/16/10...\$15.00  
DOI: <http://dx.doi.org/10.1145/2984511.2984568>

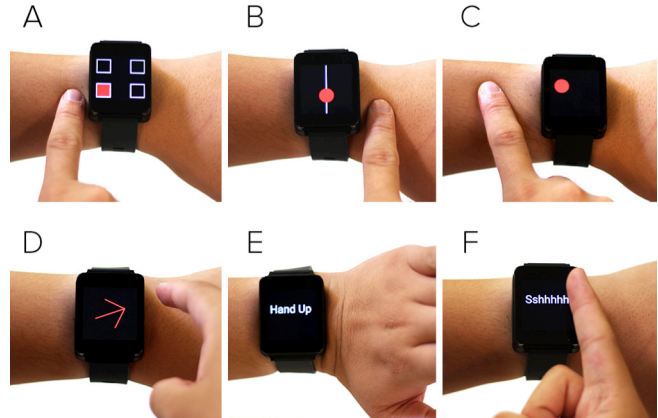


Figure 1. Six around-smartwatch modalities enabled by AuraSense: on-skin buttons (A), sliders (B) 2D trackpad (C), in-air radial input (D) and hand gestures performed on the smartwatch-bound arm (E) and other hand (F).

In this work, we describe *AuraSense*, an off-the-shelf smartwatch augmented with electric field (EF) sensing. We found EF sensing to be particularly well suited for around device interaction because of several key properties: it is fast (~200 frames per second), low-cost (~\$5), requires no additional instrumentation of the arm or finger, and finally, does not suffer from line-of-sight issues (e.g., works through clothing). The concept of using EF sensing was first proposed in Zimmerman et al. [31], however, *AuraSense* is the first work to implement and evaluate EF sensing in a watch form factor.

We were particularly inspired by Goc et al.’s work that applied electric field sensing to enhance interaction on a smartphone display [7]. They identified two useful input modalities: 1) above screen 3D tracking of finger position, and 2) coarse movement gestures above the screen, such as directional swipes. We extend this work by integrating EF sensing into a small smartwatch form factor, explore opportunities above and adjacent to the watch, demonstrate six interaction modalities (Figure 1) made possible through new electrode configurations, which can further be dynamically reconfigured for optimal sensing. Additionally, we quantify the feasibility and accuracy of the six modalities through a multi-part user study.

## RELATED WORK

Our work intersects several large bodies of literature, including smartwatch interaction techniques, around device interaction, on-body sensing, and other systems that employ electric field sensing. We now briefly review key work.

### Expanding Smartwatch Inputs

Interactions above or in close proximity to watches have been extensively explored. For example, SkinButtons [15] extended smartwatch interaction out onto the user’s arm by using small projected icons and infrared proximity sensors. Interactions above or in close proximity to watches have also been explored, for example, Abracadabra [10] and uTrack [2] use a magnetic ring and a magnetometer for in-air tracking. Ni et al. [21], Gesture Watch [12], and HoverFlow [14] enable similar interactions using infrared proximity sensors. It is also possible to capture physical touches and manipulation of the band [25], bezel [1] and watchface [28]. In general, these approaches mitigate finger occlusion and expand interaction beyond the limits of the small screen. By using EF sensing, previously unexplored in this domain, we enable more diverse and higher-fidelity interaction modalities than prior work.

### On-Skin Touch Sensing

Another approach to appropriating the skin for touch input is to overlay a sensing layer onto the skin [13,26]. However, there are also techniques that avoid direct instrumentation, including acoustic sensing [11,16,20], infrared light sensing [15,17,22], camera-driven approaches [4,9], and RF triangulation [30].

### Electric Field Sensing for HCI Applications

EF sensing is a well known technique that has been previously explored for *e.g.*, gestures [5,7,27], motion sensing [3], and even activity tracking [19]. Three configurations are common. *Loading-mode* inserts an electric signal into an electrode and measures the capacitive coupling between the electrode and an object of interest. *Transmit-mode* passes a signal through the human body; the signal is captured by a receiver electrode touched by the user. *Shunt-mode* uses emitting and receiving electrode pairs and measures the disturbance when a conductive object (*e.g.*, a finger) interferes with the electric field. Please refer to [24] for a more detailed comparison of these three configurations.

Compared with the other two configurations, *shunt-mode* offers more robust and characteristic signals, and is more compatible with a watch form factor (*i.e.* *transmit mode* would require the insertion of a signal into the non-watch hand). AuraSense operates in shunt-mode, utilizing one transmitter and four receiver electrodes. As we will discuss, we vary the size, shape and physical placement of our transmitters and receivers to instantiate different field geometries, which in turn, naturally lend themselves to different interactive uses.

## IMPLEMENTATION

Our hardware prototype uses a Microchip MGC3130 electric field sensing chip [18], costing roughly \$5, which we

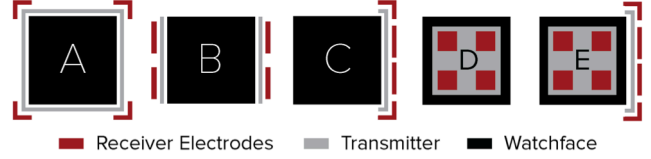


**Figure 2.** We identified four antenna configurations (A through D) that enabled interaction modalities of particular interest. These configurations have one transmitter (grey) and four receiver electrodes (red). Configuration E combines design C and D, placing an emphasis on interactions occurring to the right of the watch.

connect to various antenna configurations (Figures 2 and 3). Our setup uses one transmitter and four receiver electrodes. We use copper foil tape for our electrodes, covered by a thin layer of Mylar tape. When the transmitter and receivers are stacked, the Mylar insulates the two layers from one another. We configure the transmitter to generate an electric field by emitting a 115 kHz, 3Vpp square wave. The chip monitors each of the receiver electrodes and computes the field attenuation at 200 frames per second, which are reported to a laptop over USB for further processing.

For signal processing and machine learning, our classifier ingests 12 features. Four of these features are the raw values from the four receiver electrodes. We also compute the min and max values, as well as the mean and standard deviation, yielding four more features. We use the per-instance min and max values to normalize the four raw values, bringing the total number of features to twelve. Although we experimented with other features during development, we found that these basic features were innately discriminative and reliable for classification. For machine learning, we use SVM (SMO; kernel=RBF) and SMOReg (kernel=RBF) for classification and regression tasks respectively [8].

As a further proof of concept, we instrumented an LG G W100 Smartwatch, allowing for live input and graphical output (see Figure 1 and Video Figure).

### Antenna Design Space

Any charge-carrying surface (*e.g.*, an electrode) can generate an electric field. This field becomes distorted when a conductive object (*e.g.*, a user’s finger) becomes proximate, as portions of the electric field are drawn to the conductive object and shunted to ground. In general, EF sensing relies on detecting these field disturbances. This also means that strategic placement of the transmitter and receivers can greatly affect the geometry of the sensed region.

To this end, we experimented with a wide variety of antenna configurations. Note that our prototype is comprised of one transmitter (TX) and up to four receiver (RX) electrodes. Through rapid prototyping and testing, we found four configurations that enabled six interesting possibilities for around-smartwatch interaction. These input modalities are shown in Figure 1 and the enabling electrode geometries are shown in Figure 2. Figure 3A shows a close-up of the antenna design A. Among the successful designs, we

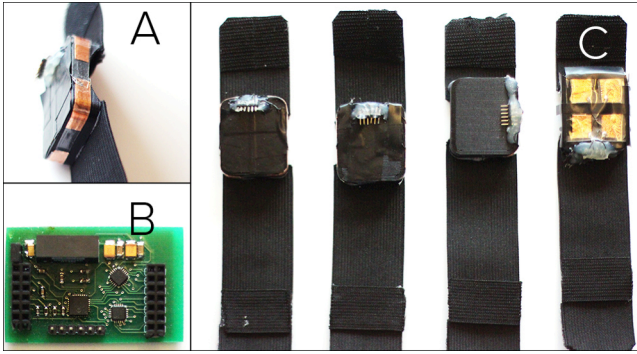


**Figure 3. A: Close-up of the antenna design A (from Figure 2). B: Our custom PCB for dynamic antenna configuration. C: Four antenna design prototypes.**

found a common scheme of placing the transmitter behind the receiver electrodes, and also using an electrode size of at least  $10 \times 6\text{mm}$ . Details on electrode geometry and placement are discussed in the following sections.

### Dynamic Antenna Configurations

Certain antenna configurations are better suited to particular input modalities. In other words, no single antenna design can support all of the interactions we developed for AuraSense. Thus, we created a prototype that featured ten electrodes (Figure 2E). This design combines elements from configurations C and D, though emphasizes interactions to the right of the watch (as opposed to being fully symmetric, which could support all six interactions). The MGC3130 chip can read a maximum of five receiver electrodes at once, and so we built a small multiplexing board (Figure 3B) that allowed us to dynamically select which electrodes are transmitters or receivers. This setup supports multiple modalities in one *unified* device, though only a single sensing modality can be active at any given time (e.g., requested by the currently active application).

### EXAMPLE INTERACTION TECHNIQUES

We now describe the six interaction modalities we found particularly promising. In addition to offering example applications, we discuss the associated antenna design, and include a targeted accuracy evaluation. These modalities are seen in Figure 1 and demonstrated in our Video Figure.

Although we discuss evaluation results individually (*i.e.*, within each modality), it was actually run as a single, monolithic study. We recruited 10 participants (2 female) with an average age of 23. The order of the evaluated interactions was randomized. For each evaluation, the corresponding antenna design prototype (Figure 3C) was worn on participants’ wrists, like a smartwatch. The watch was worn on the left, since all participants were right handed. We then trained our system with three rounds of training data, and then test *it in real time* (*i.e.*, evaluated live – no post hoc calibration, feature engineering, etc.). Any modality-specific details are discussed in their respective sections. For tasks with targets, we marked participants’ skin a non-toxic, washable marker. In total, the study took one hour.

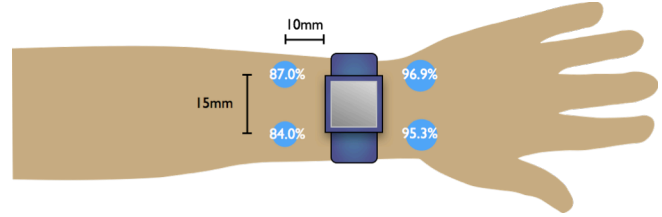


**Figure 4. Average mean errors for virtual buttons on the skin. Not touch, a fifth class, was 100% accurate.**

### Buttons on the Skin

This modality places four virtual “buttons” on the skin (*i.e.*, the same as Skin buttons [15]), two on each side of the watch, as illustrated in Figure 1A and 4. Using antenna design B—which pairs one virtual button to one receiver—we can sense whether a finger has clicked a skin-bound button.

For the evaluation, we marked the skin surrounding our prototype watch with four crosshairs, located 10mm from the side of the watch and separated 15mm vertically (as illustrated in Figure 4). We trained the system by having participants click the crosshairs one time each, in a random order, three training rounds. We then trained a five-class SVM – one class for each of the *four buttons* and fifth class for *no touch*. In round four, tested live, the four buttons were 92.7% accurate, (SD=7.0%) with *no touch* achieving 100% accuracy.

### Sliders on the Skin

We found that placing all four receivers on one side of the watch (Figure 2, antenna design C) enabled high fidelity, continuous sensing on that side. This is well suited for absolute or relative scrolling or sliding along the skin directly next to the watch face (Figure 1B).

To evaluate this input modality and antenna configuration, we drew a 40mm long line on participants’ skin, parallel to the left side of the watch, offset by 10mm. We then marked this line with four ticks spaced 10mm apart vertically, numbered 1 through 5. A round of data collection consisted of a user placing a finger on an announced tick number, after which one trial was recorded. Participants were then asked to slide the finger to another tick number (random order). The tick number and EF sensed features were used to train a SVM regression model (RBF kernel,  $\gamma=0.6$ ). The fourth round, which followed the same process as above, tested the accuracy live, and showed a mean absolute distance error of 2.0mm (SD=2.0mm).

### Trackpad on the Skin

We also used antenna design C to see if it was possible to support not just 1D finger tracking—as discussed in the previous section—but also 2D tracking, like a trackpad on the skin (Figure 1C).

To evaluate this modality, we drew a  $3 \times 3$  pattern of crosshairs to the left of the watch (offset 10mm from the watch, with a grid spacing of 10mm, illustrated in Figure 5). As before, we collected three rounds of training data, with each



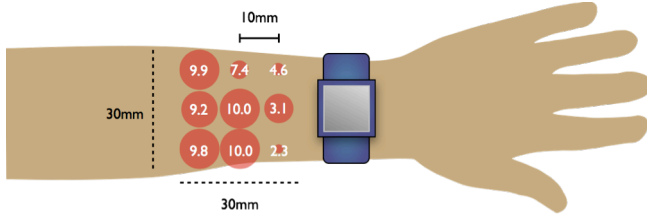


**Figure 5. Tracking accuracy across a  $3 \times 3$  grid. The circles represent the average mean error, and are rendered to scale.**

round consisting of a single touch to each crosshair (random order). In this case, two SVM regression models (RBF kernel,  $\gamma=0.6$ ) were trained – one for X-axis tracking, and another for the Y-axis. Finally, we evaluated the regression accuracy in a live test. The results, depicted in Figure 5, reveal a mean distance error of 7.2mm (SD=6.0mm).

### Radial Input

The three previous modalities all utilize the skin as a physical surface on which interactions can be triggered. However, it is equally possible to utilize the free-space around the watch for interaction. In this modality, we consider radial input (Figure 1D) around the periphery of the watch (similar to e.g., Abracadabra [9], but which required a magnetic ring). We found that antenna design D, which featured four upward-facing receivers arranged in a grid, performed best.

To evaluate this modality and design, we asked participants to position a finger at one of eight possible angles ( $45^\circ$ ,  $90^\circ$ ,  $135^\circ$ , ...  $360^\circ$ ), requested once each, in a random order. Three rounds of data were collected and used to train a single SVM regression model (RBF kernel,  $\gamma=0.3$ ). We then ran an identical procedure, but recorded the live classification output, which resulted in an average angular error of  $18.0^\circ$  (SD= $20.1^\circ$ ).

### Smartwatch-Arm Hand Gestures

When experimenting with antenna design A, we found that movements of the hand on the *same* arm as the smartwatch (i.e., the “smartwatch-arm”) affected the EF signal. In response, we explored the feasibility of supporting static hand poses (Figure 1E), which could operate in parallel with the previously describe techniques. This is inline with previous work [6,23,29] that detects hand gestures for smartwatch manipulation. We built an exemplary hand gesture set, seen in Figure 6 (top row).

To test accuracy, we had participants perform each of the hand gestures in a random order (i.e., one round of data collection). We then repeated this process for two more rounds. We used this collected data to train a multi-class SVM (RBF kernel,  $\gamma=0.7$ ). As usual, we used round four to test the accuracy live. Overall, the gesture set achieved a mean accuracy of 88.8% (SD=8.15%).

### Free-Arm Hand Gestures

It is also possible to use the other hand (i.e., *non-smartwatch-arm*) for gestural input above the watch face (Figure 1F). This interaction has been shown in previous

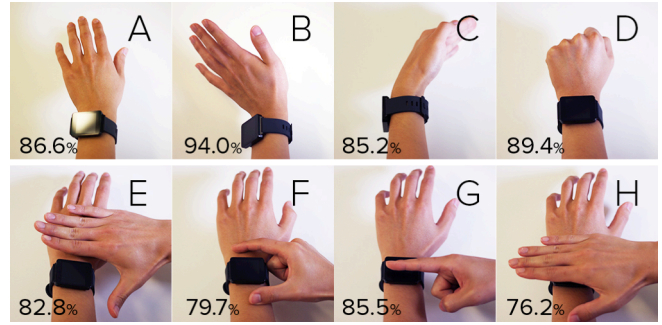


**Figure 6. Our “smartwatch-arm” (top) and “free-arm” (bottom) gesture sets. Per-gesture recognition accuracies inset.**

work using other sensing methods [12,14]. We found that antenna D, also used for radial input, offered the most responsive and distinctive signal. We developed a different hand gesture set, shown in Figure 6 (bottom row). Using the exact same procedure as the previous study, we found a mean gesture recognition accuracy of 82.8% (SD=13.3%).

### EXAMPLE USES

The input modalities we described could be used to power a wide variety of interactive applications on smartwatches. For example, when the screen is off, AuraSense could anticipate the user is ready for interaction (e.g., detecting nearby finger), and automatically activate the display. With the screen now active, the user could circle his finger above the watchface (*radial input*) to browse different applications. Touching the screen would launch the selected item. In addition to manual selection, the user could also launch global actions with “letter gestures”. For example, drawing an “M” on the skin (*trackpad*) could launch a music app.

When in the music app, on-screen buttons (ones too small for accurate finger presses) could be located on the sides of the interface. The user can press, e.g., “playlists”, by tapping the skin adjacent to the label (*buttons*). To browse songs in the playlist, the user could scroll up and down on the skin (*slider*). Tapping the screen would start playing the selected song. To move backwards or forwards through playlists, users could perform “flap up” or “flap down” gestures with the *smartwatch arm* (Figure 6, B & C). If a phone call comes in, the user can perform a “shhh” (Figure 6G) gesture using the *free arm* to silence the incoming call.

### LIMITATIONS

One of the most significant limitations of our setup was signal drift. Specifically, the MGC3130 chip obtains relative electric field readings based on parameters captured during an initial calibration procedure. Over time (on the order of minutes), the signal begins to drift and an undesirable offset is produced. To mitigate this issue, it may be possible to use an adaptive baseline, or perhaps machine learning features that are based on relative values between electrodes, rather than absolute values. Additionally, EF sensing is also susceptible to ambient electrical noise, such as environmental EM noise. Adaptive background subtrac-

tion might help mitigate this issue. Finally, the small form factor of a smartwatch limits electrode size and also the maximum distance between transmitter and receiver pairs. We found this generally limited finger sensing range to a few centimeters, permitting only close interactions.

## CONCLUSION

*AuraSense* is a technique for supporting multiple around-device interaction modalities on smartwatches using electric field sensing. Although this sensing technique has been widely used, we are the first to use it for worn input with a smartwatch form factor. To explore the design space, we prototyped a variety of antenna configurations and identified four designs that enabled previously identified, promising input modalities. We built several prototypes, including one that can dynamically switch between different antenna configurations, thus enabling high fidelity sensing for a particular input modality. Finally, we conducted a multi-part user study to help quantify the basic feasibility and accuracy of the six example interaction modalities.

## ACKNOWLEDGEMENTS

This research was generously supported by the David and Lucile Packard Foundation, a Google Faculty Research Award, and Qualcomm.

## REFERENCES

1. Ashbrook, D., Lyons, K. and Starner, T. An investigation into round touchscreen wristwatch interaction. In *Proc. MobileHCI '08*, 311-314.
2. Chen, K., Lyons, K., White, S. and Patel, S. N. uTrack: 3D input using two magnetic sensors. In *Proc. UIST '13*, 237-244.
3. Cohn, G., Gupta, S., Lee, T., Morris, D., Smith, J.R., Reynolds, M.S., Tan, D.S. and Patel, S.N. An ultra-low-power human body motion sensor using static electric field sensing. In *Proc. UbiComp '12*, 99-102.
4. Dezfuli, N., Khalilbeigi, M., Huber, J., Müller, F. and Mühlhäuser, M. PalmRC: imaginary palm-based remote control for eyes-free television interaction. In *Proc. EuroITV '12*, 27-34.
5. Endres, C., Schwartz, T. and Müller, C.A. Geremin: 2D microgestures for drivers based on electric field sensing. In *Proc. IUI '11*, 327-330.
6. Fukui, R., Watanabe, M., Gyota, T., Shimosaka, M. and Sato, T. Hand shape classification with a wrist contour sensor. In *Proc. UbiComp '11*, 311-314.
7. Goc, M.L., Taylor, S., Izadi, S. and Keskin, C. A low-cost transparent electric field sensor for 3d interaction on mobile devices. In *Proc. CHI '14*, 3167-3170.
8. Hall, M., Frank, E., Holmes, G., Pfahringer, B., Reutemann, P. and Witten, I.H. The WEKA Data Mining Software: An Update; In *SIGKDD Explorations*, 11(1).
9. Harrison, C., Benko, H. and Wilson, A.D. OmniTouch: wearable multitouch interaction everywhere. In *Proc. UIST '11*, 441-450.
10. Harrison, C. and Hudson, S.E. Abracadabra: wireless, high-precision, and unpowered finger input for very small mobile devices. In *Proc. UIST '09*, 121-124.
11. Harrison, C., Tan, D. and Morris, D. Skinput: appropriating the body as an input surface. In *Proc. CHI '10*, 453-462.
12. Kim, J., He, J., Lyons, K. and Starner, T. The Gesture Watch: A Wireless Contact-free Gesture based Wrist Interface. In *Proc. ISWC '07*, 1-8.
13. Kramer, R., Majidi, C. and Wood, R. Wearable tactile keypad with stretchable artificial skin. In *Proc. ICRA '11*, 1103-1107.
14. Kratz, S. and Rohs, M. Hoverflow: exploring around-device interaction with IR distance sensors. In *Proc. MobileHCI '09*. Article 42, 4 pages.
15. Laput, G., Xiao, R., Chen, X., Hudson, S.E. and Harrison, C. Skin buttons: cheap, small, low-powered and clickable fixed-icon laser projectors. In *Proc. UIST '14*, 389-394.
16. Liang, R., Lin, S., Su, C., Cheng, K., Chen, B. and Yang, D. SonarWatch: appropriating the forearm as a slider bar. In *Proc. SIGGRAPH Asia Emerging Technologies*. Article 5, 1 page.
17. Lim, S.C., Shin, J., Kim, S.C. and Park, J. Expansion of Smartwatch Touch Interface from Touchscreen to Around Device Interface Using Infrared Line Image Sensors. *Sensors* 2015, 15, 16642-16653.
18. Microchip Technology Inc. MGC3030/3130 3D Tracking and Gesture Controller Data Sheet. <http://ww1.microchip.com/downloads/en/DeviceDoc/40001667D.pdf> Last Retrieved: July 25, 2016
19. Mujibiya, A. and Rekimoto, J. Mirage: exploring interaction modalities using off-body static electric field sensing. In *Proc. UIST '13*, 211-220.
20. Mujibiya, A., Cao, X., Tan, D.S., Dan Morris, Patel, S. S. and Rekimoto, J. The sound of touch: on-body touch and gesture sensing based on transdermal ultrasound propagation. In *Proc. ITS '13*, 189-198.
21. Ni, T. and Baudisch, T. Disappearing mobile devices. In *Proc. UIST '09*, 101-110.
22. Ogata, M., Sugiura, Y., Makino, Y., Inami, M. and Imai, M. SenSkin: adapting skin as a soft interface. In *Proc. UIST '13*, 539-544.
23. Rekimoto, J. GestureWrist and GesturePad: Unobtrusive Wearable Interaction Devices. In *Proc. ISWC '01*, 21-27.

24. Smith, J., White, T., Dodge, C., Paradiso, J., Gershenfeld, N. and Allport, D. Electric field sensing for graphical interfaces. *IEEE Computer Graphics and Applications*, vol. 18, no. 3, pp. 54-60.
25. Simon, P.T., Lecolinet, E., Eagan, J. and Guiard, Y. Watchit: simple gestures and eyes-free interaction for wristwatches and bracelets. In *Proc. CHI '13*, 1451-1460.
26. Weigel, M., Lu, T., Bailly, G., Oulasvirta, A., Majidi, C. and Steimle, J. iSkin: Flexible, Stretchable and Visually Customizable On-Body Touch Sensors for Mobile Computing. In *Proc. CHI '15*, 2991-3000.
27. Wilhelm, M., Krakowczyk, D., Trollmann, F. and Albayrak, S. eRing: multiple finger gesture recognition with one ring using an electric field. In *Proc. WOAR '15*, Article 7, 6 pages.
28. Xiao, R., Laput, G. and Harrison, C. Expanding the input expressivity of smartwatches with mechanical pan, twist, tilt and click. In *Proc. CHI '14*, 193-196.
29. Zhang, Y. and Harrison, C. Tomo: Wearable, Low-Cost Electrical Impedance Tomography for Hand Gesture Recognition. In *Proc. UIST '15*, 167-173.
30. Zhang, Y., Zhou, J., Laput, G. and Harrison, C. Skin-Track: Using the Body as an Electrical Waveguide for Continuous Finger Tracking on the Skin. In *Proc. CHI '16*, 1491-1503.
31. Zimmerman, T.G., Smith, J.R., Paradiso, J.A., Allport, D and Gershenfeld, N. Applying electric field sensing to human-computer interfaces. In *Proc. CHI '95*, 280-287.